We are IntechOpen,
the world's leading publisher of
Open Access books
Built by scientists, for scientists

6,900
Open access books available

186,000
International authors and editors

200M
Downloads

Our authors are among the

154
Countries delivered to

TOP 1%
most cited scientists

12.2%
Contributors from top 500 universities

CLARIVATE ANALYTICS
BOOK CITATION INDEX
INDEXED

WEB OF SCIENCE™

Selection of our books indexed in the Book Citation Index
in Web of Science™ Core Collection (BKCI)

Interested in publishing with us?
Contact book.department@intechopen.com

Satellite Control System: Part I - Architecture and Main Components

Yuri V. Kim

Abstract

This chapter provides introductory material to satellite control system (SCS). It is based on the author's experience, who has been working in areas of SCS development, including designing, testing, operating of real SCS, as well as reviewing and overseeing various SCS projects. It briefly presents SCS generic futures and functional principles: tasks, architecture, basic components and algorithms, operational modes, simulation and testing. The chapter is divided into two parts, namely, Part I: SCS Architecture and Main Components and Part II: SCS Simulation, Control Modes, Power, Interface and Testing. This chapter focuses on Part I. Part II will be presented as a separate chapter in this book.

Keywords: satellite control, attitude and orbit, determination, estimation, sensors, actuators, coordinate systems, reference frame, state estimation and Kalman filtering, earth gravity, magnetic fields

1. Introduction

Satellite control system (SCS) is a core, essential subsystem that provides to the satellite capabilities to control its orbit and attitude with a certain performance that is required for satellite mission and proper functioning of satellite payload operation. However, the first mandatory task for SCS is assuring satellite safe functionality; providing sufficient electric power, thermal and communication conditions to be able for nominal functioning during specified life time at different sun lightening conditions (including potential eclipse periods), protecting against life critical failures proving to satellite safe attitude in Safe Hold Mode (SHM). Without SCS or satellite guidance, navigation and control (GN&C) system, any Earth-orbiting satellite could be considered just as artificial space body, demonstrating the *launcher* capability for the satellite launch. As soon as a satellite is assigned to perform a certain space mission, it has to have SCS and a kind of special device (s)-payload (s), performing scientific, commercial or military tasks that are dedicated to this mission. Today, the widespread satellite and SCS design philosophy [1–3] is based on the concept that satellite is a platform (bus or transportation vehicle) for the very important person (VIP) passenger, which is the payload, and this platform is aimed just to deliver and carry it in space. This approach has been proven as successful or, at least, satisfactory from the commercial point of view. However, the first Soviet satellite "Sputnik" and further Soviet/Russian satellites

were built and launched under the different philosophy that satellite is the main "personage" performing a space mission and the payload (unlikely the ballistic rocket war head (s)) is just one of the satellite subsystems that should be integrated into the satellite board under the satellite chief designer guidance, who is responsible for the mission performance. From the author's point of view, this approach has certain advantages following from the Aerospace System Engineering, integration and distribution functions, and responsibilities between the space mission participants. In this chapter, SCS is presented from this point of view, integrating conventionally separate satellite GN and C subsystems and devices into the joint integrated system, attitude and orbit determination and control system (AODCS). The main principles and features of this system are presented in this chapter.

2. Earth-orbiting satellites and the role of the control system

The first human-made Earth-orbiting satellite (Soviet Sputnik), Simplest Satellite (SS-1), was launched on October 4, 1957. This satellite was launched following the development of the Soviet intercontinental ballistic rocket R-7 (8 K71). Nevertheless, it started a new era of space human exploration (**Figure 1**).

SS-1 technical characteristics are as follows [4, 5]:

- Mass 83.6 kg; sealed from two identical hemispheres with a diameter of 0.58 m; life time 3 months; payload, two 1 W transmitters (HF, 20.005 and VHF, 40.002 MHz) with four unidirectional deployable antennas (four 2.4–2.9 m metallic rods); electrical batteries, silver-zinc; sufficient for 2 weeks.

- Orbit: perigee 215 km, apogee 939 km, period 96.2 min, eccentricity 0.05, inclination angle 65.10 deg.

- Inside, the satellite sphere was filled by nitrogen, and the temperature was kept within 20–23 deg. C with automatic thermoregulation-ventilation system (thermometer-ventilator).

- The satellite had no attitude control and was free rotated around its center of mass in orbit, keeping initial angular speed, provided by the separation pulse after the separation from the launch rocket. However, thanks to the four rod

SS1 launch rocket General Designer

S.Korolev (R-7)

SS1 Lead Designer

M. Homiakov

Figure 1.
*Soviet designers-creators of the first earth-orbiting artificial satellite SS-1.*

antennas that provided unidirectional radio transmission in the two-radio bends, HF and VHF, SS-1 evidently indicated its presence in space for all people over the world. Even amateur radio operators with amateur receivers could receive famous now signals: BIP, BIP, BIP ... !! (**Figure 2**).

Figure 2.
SS-1, assembled (left). Open two semispheres (right).

Since SS-1, about 8378 satellites were launched to year 2018 [6]. Early satellite launches were extraordinary events and demonstrated tremendous achievement of the launched state, the USSR (4 Oct. 1957, SS-1), the USA (31 Jan. 1958, Explorer 1) and Canada (29 Sep. 1962, Alouette, launched by Thor-Agena, a US two-stage rocket), but with time, satellite launches became ordinary and usually pursue a certain military or civil mission.

Among the civil missions (satellites), the following types can be determined as already conventional: navigation, communication, Earth observation, scientific, geophysics and geodetic, technology demonstration and developers training. These satellites are usually equipped with a kind of payload system(s) (radio/TV transmitter/transducer, radar, telescope or different scientific instrument, etc.) to perform certain dedicated space mission(s). For example, the first Canadian Earth observation satellite RADARSAT-1 (Nov 4, 1995–May 10, 2013; **Figure 3**) was equipped with a side-looking synthetic aperture radar (SAR) on board the International Space Station (November 1998, ISS; **Figure 4**) was installed a Canadian robotic arm for its assembling and maintenance.
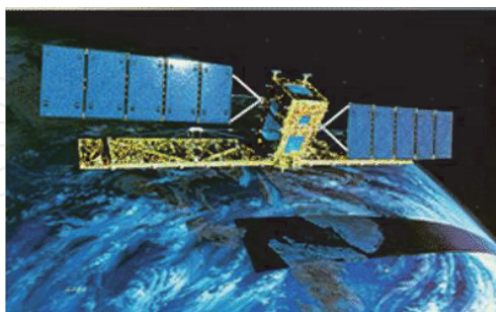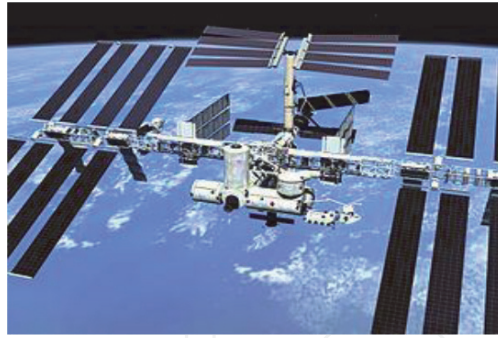

Figure 3.
*The first Canadian earth observation satellite RADARSAT-1.*

According to the satellite altitude (h), their orbits can be classified as low-altitude (LEO), 200–2000 km; medium-altitude (MEO), 5000–20,000 km; and high-altitude (HEO), h > 20,000 km; according to eccentricity as: close to circular e < 0.01; elliptical 0.01 < e < 0.3; highly elliptical 0.3 < e < 0.8.

There are satellites with special type of orbit such as polar (i = 90 deg), equatorial geostationary (GEO, i = 0 and h = 35,800 km) and Sun-synchronous provide orbital precession equal to Sun annual rate (i depends on satellite period) (**Figure 5**).

Figure 4.
International Space Station (ISS).
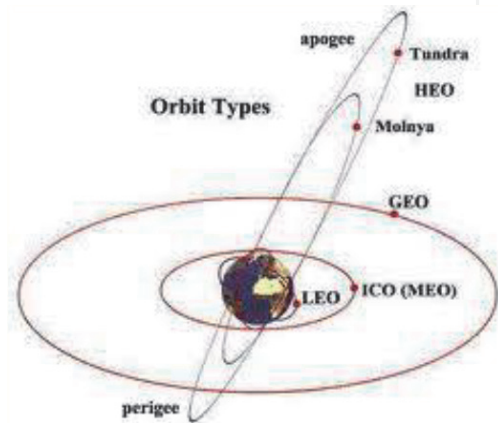
Figure 5.
Satellite orbit types ("tundra" and "Molniya" are Russian communication satellites in highly ecliptic orbits).

Miniaturized low-cost satellites are as follows: small satellites (100–500 kg), microsatellite (below 100 kg) and nanosatellite (below 10 kg).

A large diversity of satellites serving for different missions is in space now. A widespread point of vew is that all of them are transportation platforms delivering and carrying in orbit dedicated to the planned space mission payload system, like a VIP passenger. For example, it could be the postman for the postal horse carriage for many years ago. Namely, the satellite with its control system (SCS) provides to the payload all conditions required for the mission performance (orbit, attitude, power, pressure, temperature, radiation protection and communication with ground mission control center (MCC)). That is why from the mission integration point of view, the SCS can be seen as the space segment integration bases that set their development and operation process in corresponding order. In turn, SCS as satellite subsystem also can be reviled and established in satellite onboard equipment architecture, combining the group of subsystems that are dedicated to orbit and attitude determination and control tasks. It could be done rather from the System Engineering than from the commercial practice point of view and would significantly streamline satellite development order and the degree of responsibility of all the developers.

It should be mentioned that such group of aircraft equipment in aviation has been named as GN&C Avionics; hence, for space, it can be named as the *Spacetronics*, and the heritage of system development and integration wherever it is possible should be kept. Essential difference with Avionics for the Spacetronics is that it should work for specified life time in space environment (dedicated orbit) after mechanical start-up impacts (overload, vibration) connected to the launch into the orbit. The verification of this capability is usually gained in special space qualification ground tests that imitate launch impact and space environment with thermo-vacuum and radiation chambers, mechanical load and vibration stands [7, 8].

3. Satellite control system architecture and components

3.1 SCS architecture

Today, for many satellites, GN&C onboard equipment can be presented by the following subsystems, performing related functions listed below:

- Global Positioning System (GPS)—onboard satellite orbit and time determination

- Propulsion system—orbit/attitude control system

- Attitude Determination and Control System (ADCS)—satellite attitude determination and control

Integration of these subsystems can be named as *attitude and orbit determination and control system or Spacetronic system.* Typically, AODCS includes the following components:

- Onboard computer system (OBCS) or dedicated to AODCS electronic cards (plates) in Central Satellite Computer System (e.g., command and data handling computer (C&DH))

- Sensors

- Actuators

Basic AODCS architecture is presented in **Figure 6**.

OBCS, onboard computer system; TLM, telemetry data and commands; PL, payload; PS, propulsion system; RW, inertia reaction wheels; MTR, magnetic torque rods; GPS, satellite navigation Global Positioning System; MAG, 3-axis magnetometer; SS, 2-axis Sun sensor; HS, horizontal plane sensor; ST, star tracker; RS, angular rate sensor; EP, electric power; TR, temperature regulation; VP, vacuumed protection; RP, radiation protection.
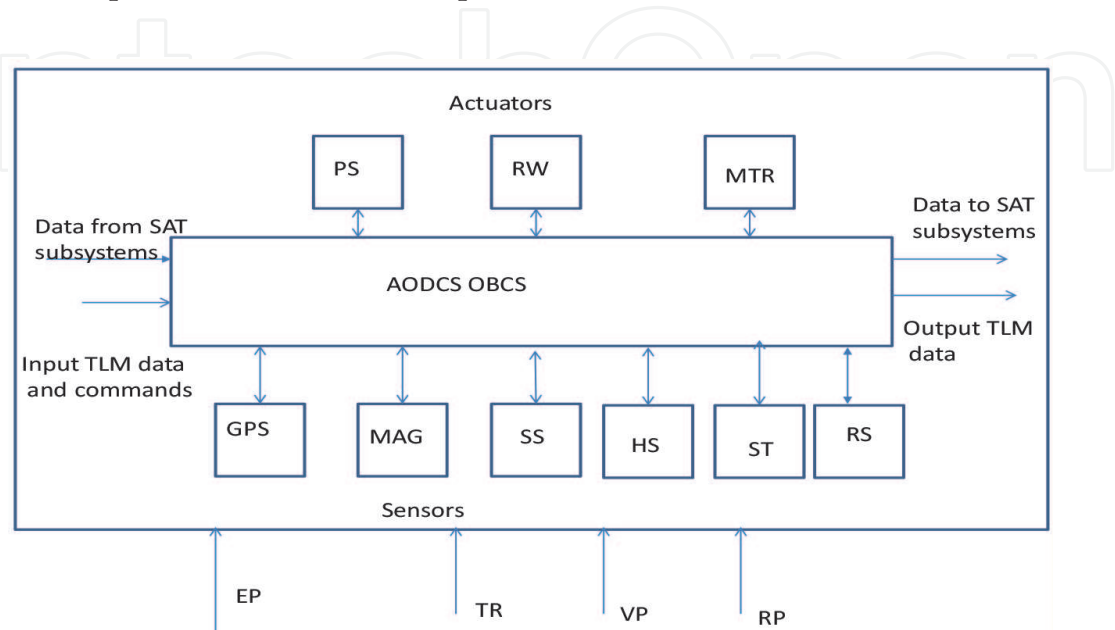
Figure 6.
Satellite AODCS system.

Depending on required reliability and life time, each component can be a single or redundant unit. Unlike airplanes, satellite is an inhabitant space vehicle that is operated from the ground. The operation is usually performed via a bidirectional telemetry radio link (TLM) in S-band (2.0–2.2 GHz). Payload data downlink radio link (unidirectional) is usually performed via X-band (7.25–7.75 GHz;). For both links, usually the same data protocol standards are applied **Figure** 7.
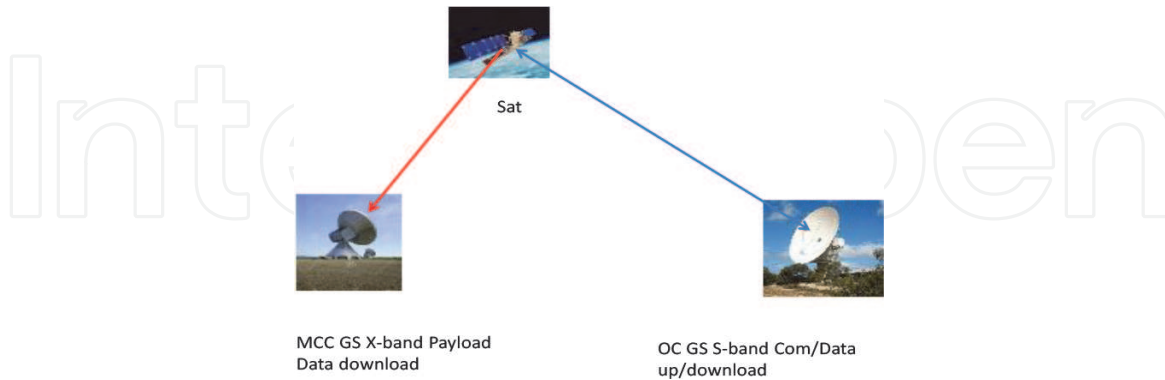
Figure 7.
Satellite communications with ground stations.

Two subsystems can be allocated in AODCS architecture, namely, orbit determination and control subsystem (ODCS) and attitude determination and control subsystem (ADCS). Practically both subsystems are dynamically uncoupled; however, orbital control requires the satellite to have a certain attitude (as well as orbital knowledge itself), and attitude control requires orbit knowledge also. Hence, orbit (its knowledge) is essentially continuously required on satellite board where it is propagated by special orbit propagator (OP). Due to orbital perturbations (residual atmospheric drag, gravity and magnetic disturbances and solar pressure), satellite orbit changes over time and OP accumulates errors; its accuracy is degraded.

Before the application of satellite onboard GPS receivers, the satellite position and velocity were periodically determined on ground by the ground tracking radio stations (GS, dish antenna), and calculated on-ground orbital parameters were periodically uploaded to satellite OBCS to correct OP, to provide available accuracy. Now with GPS satellite, orbit can be calculated onboard autonomously, and OP can propagate data only during relatively short GPS outage periods. For some applications, orbital data uploaded from the ground still can be used, at least, for fusion with GPS-based OP.

For newly developed satellites with GPS, orbit maneuvers (correction, deorbiting, collision avoidance, special formation flying and orbit servicing missions) can be executed autonomously onboard at planned time or from ground operators using orbital knowledge and TLM commands to activate satellite orbit control thrusters.

3.2 AODCS components

Below AODCS components are presented to show their generic principles that can help for the system understanding and modeling. Generic design requirements are presented in [3]. Some design examples can be found in many sources, for example, [1, 9–12].

3.2.1 Sensors

AODCS sensors are designed to measure satellite orbital and attitude position and velocity. From the most general point of view, they can be considered as the

vector measuring devices (VMD). The device can measure in space a physical vector $\overline{R}_m$ that can be known (referenced) in a reference coordinate system $\overline{R}_r$. Three parameters can be measured: vector module R and two angles of its orientation Az and El (**Figure 8**).
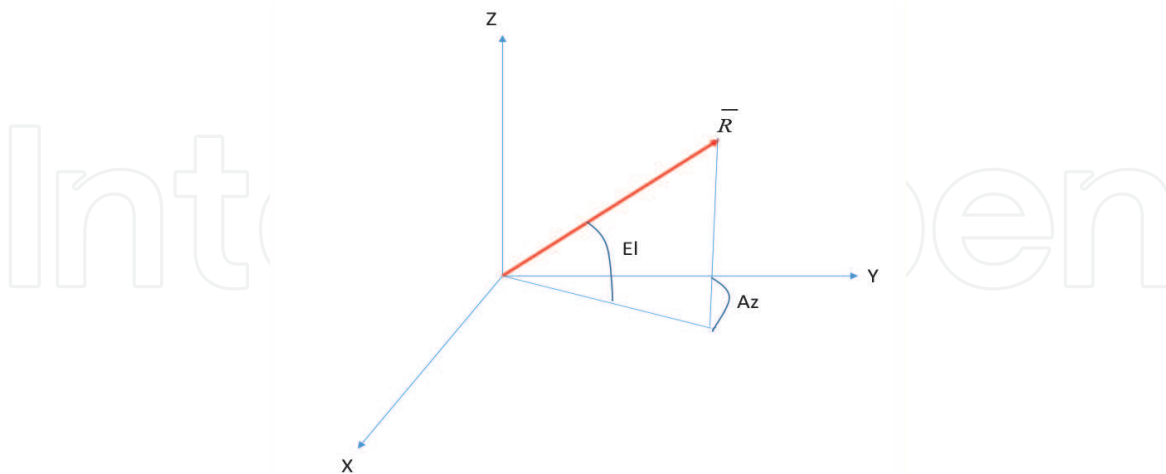
Figure 8.
Vector $\overline{R}$ in the Cartesian coordinate system XYZ.

Vector module and its orientation can be expressed as functions of its projections R_x, R_y, R_z as follows:

$$R = \sqrt{R_x^2 + R_y^2 + R_z^2}$$
$$A_z = \tan^{-1} \frac{R_x}{R_y} \qquad (1)$$
$$El = \tan^{-1} \frac{R_z}{\sqrt{R_x^2 + R_y^2}}$$

It can be noted that measurement of referenced vectors can be used for the determination of satellite position or angular orientation. A minimum of three vectors is required to determine satellite position and two to determine its attitude. If more vectors are measured providing informational redundancy, then such statistical estimation methods as least square method (LSM) and Kalman filter (KF) can be applied. Satellite velocity and angular rate can be derived by the differentiation of its position and attitude applying a kind of filter recommended by the filtering and estimation theory [13–15]. It should also be noted that if vector orientation is measured for the position determination, then satellite attitude should be known and vice versa.

Especial autonomous satellite navigation system (sensor) is the inertial navigation system (INS/inertial measurement unit (IMU)). It can be used for the determination of satellite position, velocity, orientation and angular rate simultaneously. INS is based on measuring with linear accelerometers and angular rate sensors ("gyros") the two vectors: satellite linear active acceleration $\overline{a}$ and angular rate $\overline{\omega}$. After integration, the system provides satellite position, velocity, attitude and angular rate. It is also assumed in INS theory that the vector of Earth gravity acceleration $\overline{g}$ is not measured by the system accelerometers, but it is computed from referenced mathematical Earth gravity field model. Essential INS disadvantage is that its errors grow with time. That is why, it has to be periodically corrected by such navigation aids as a pair of VMD used for the direct attitude determination. A detailed system description is out of this chapter's scope and can be found in many publications [16–18]. Only the use of
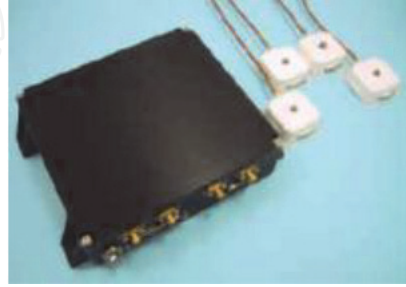
angular rate sensors ("gyros") for determination of satellite attitude is briefly considered below.

3.2.1.1 Determination of satellite position and velocity (GPS)

Today, satellite GPS can provide onboard accurate data about position, velocity and time [19] (**Figure 9**).

Accuracy: position, 15 m (2σ); velocity, 1.5 m/s (2σ); time, 1 μS.

Figure 9.
Satellite GPS SRG-10. Double redundant with a pair of zenith and nadir antennas.

GPS receiver is a radio range measuring device that measures distance from the desired satellite to navigation satellite constellation (NAVSTAR, USA; GLONASS, Russia; and GALILEO, Europe) and computes its position and velocity. GPS measures the distance R $(R = \sqrt{R_x^2 + R_y^2 + R_z^2})$ of the vector from the desired satellite to the navigation satellite, and this system is invariant of the system orientation (satellite attitude). The distance between the desired satellite and navigation satellite is measured by measuring the time delay Δt between the time t^s of the radio pulse transmitted by navigation satellite and the reception time t^r of its reception by GPS receiver installed on the desired satellite $\Delta t = t^r - t^s$. Measuring the distance allows to determine the desired satellite relative position (relatively to navigation satellite), and using known navigation satellite position that is continuously received by the receiver for every tracking satellite in the navigation message (NM) converts it in absolute position.

A minimum of three navigation satellites should be simultaneously traced by the receiver to determine position and velocity. Then satellite position is the cross-point of three spherical surfaces of the position equation $R^i = const, \ i = 1, 2, 3$. If more tracked satellites are available, then redundant information can be used to calibrate the onboard clock (using the four satellites) and to use least square method or Kalman filter. Four nonlinear algebraic equations (pseudo-range measurements) are usually used to determine satellite position with GPS receiver:

$$R^i = \sqrt{(x - x^i)^2 + (y - y^i)^2 + (z - z^i)^2} + c\tau$$

$$i = 1, 2, 3, 4$$

(2)

where R^i is the distance (pseudo-range) to the ith tracked navigation satellite, x^i, y^i, z^i are the navigation satellite Cartesian coordinates received in the NM, x, y, z are the Cartesian coordinates of the desired satellite, $c = 299\ 792\ 458\ km/s$ is the speed velocity and τ is the GPS receiver clock bias. Satellite position can be found by solving it (1) numerically. It could also be linearized by using redundant

measurements ($t > 4$) with LSM or KF. Satellite velocity can be determined by the differentiation of its position. Finally, GPS receiver can provide to AODC OBC current satellite position and velocity in the reference (e.g., Earth-centered inertial (ECI) [14] frame x, y, z, V_x, V_y, V_z and synchronized (by GPS) onboard time t^s).

3.2.1.2 Determination of satellite attitude and angular rate

3.2.1.2.1 TRIAD method (MAG, SS, HS)

The TRIAD method [10] is applied when two different vectors are measured. They usually can be any of the three pairs combined with the following three vectors: Earth magnetic induction vector $\overline{B}$ (measured with three-axis MAG), Sun vector $\overline{S}$ (measured with two-axis SS), and local vertical $\overline{r}$ (perpendicular to the local infrared radiation temperature surface, measured with the HS). At least two different not collinear vectors (their orientation) should be measured to determine satellite attitude that here is considered as satellite directional cosine matrix (DCM) and related three Euler angles of the certain order of rotations (e.g., 3-2-1) [9, 10] .

Let us assume that two different physical nature not collinear vectors $\overline{U} = \overline{S}$ and $\overline{V} = \overline{r}$ are measured $\overline{U}_m, \overline{V}_m$ by two vector measuring devises (SS and HS) installed on the satellite board and both these vectors are referenced in the reference frame as $\overline{U}_r, \overline{V}_r$. Let us choose $\overline{U}$ as the main vector and $\overline{V}$ as an auxiliary vector. Then an orthogonal coordinate system (frame) with basis unit vectors, $\overline{q}, \overline{r}$ and $\overline{s}$ can be defined as follows [10, 20]:

$$\vec{q} = \frac{\vec{U}}{|\vec{U}|}$$

$$\vec{r} = \frac{\vec{U} \times \vec{V}}{|\vec{U} \times \vec{V}|} \tag{3}$$

$$\vec{s} = \vec{q} \times \vec{r}$$

These unit vectors expressed at a given time by measured values in measured frame or body frame and reference values in a reference frame define two rotation matrixes, $\mathbf{C_m}$ and $\mathbf{C_r}$, as follows:

$$\mathbf{C_m} = \left[\mathbf{q_m}; \mathbf{r_m}; \mathbf{s_m} \right]$$

$$\mathbf{C_r} = \left[\mathbf{q_r}; \ \mathbf{r_r}; \ \mathbf{s_r} \right] \tag{4}$$

where vectors $\overline{q}, \overline{r}, \overline{s}$ are written in the matrix form as matrix columns.

Rotation matrix C_{br} that defines attitude in the body frame with respect to reference frame is determined by the following formula:

$$\mathbf{C_{br}} = \mathbf{C_m} \cdot \mathbf{C_r} \tag{5}$$

Three Euler angles of rotation, roll (ϕ), pitch (θ), and yaw (ψ), can be expressed through the elements of the matrix C_{br}. Certain trigonometric formulas depend on the agreement about the order of the body rotations. For the order 3-2-1, the matrix C_{br} is as follows [9, 10]:

$$\mathbf{C_{br}} = \begin{bmatrix} c\theta c\psi & c\theta s\psi & -s\theta \\ s\phi s\theta c\psi - c\phi s\psi & s\phi s\theta s\psi + c\phi c\psi & s\phi c\theta \\ c\phi s\theta c\psi + s\phi s\psi & c\phi s\theta s\psi - s\phi c\psi & c\phi c\theta \end{bmatrix} \tag{6}$$

where c and s stand for cosine and sine angle. Then, formulas for Euler angles can be derived from (6) as:

$$\begin{aligned} \phi &= \tan^{-1}\frac{C_{23}}{C_{33}}, \\ \theta &= -\sin^{-1}C_{13}, \\ \psi &= \tan^{-1}\frac{C_{12}}{C_{11}} \end{aligned} \tag{7}$$

Vector measured sensors

If a pair from the three vectors (B, S, r-write as vectors) is measured, then following VMD in the pair can be used: SS (**Figure 10**), HS (**Figure 11**) and MAG (**Figure 12**).

Figure 10.
S-vector sensor Bradford fine sun sensor, accuracy, 0.2 deg. (2σ).

Figure 11.
r-vector sensor HS CMOS/SRAM-modular infrared horizon sensor, accuracy, 0.4 deg. (2σ).

Figure 12.
B-vector sensor MAG TFM100-S, accuracy, 10mG (2σ).

3.2.1.2.2 LSM method for star tracker (ST)

If more than two vectors are measured and available for attitude determination, then LSM-BATCH method [10] can be applied to use informational redundancy for

increasing the stochastic estimation accuracy. This method basically can be applied for any set of VMD but is specifically convenient for the star tracker (ST), when some number (n) of navigation stars are in the device field of view (FOV) and are detected and tracked simultaneously, providing measured vectors $\overline{R}_m$ to these stars that are referenced in the device space catalog $\overline{R}_r$ (**Figures 10–13**).

Figure 13.
Star direction R-vector measured sensor (optic and computer units). Advanced stellar compass, accuracy,
$2'' - 16''$ (2σ).

Let us consider the transformation of the referenced vector $\overline{R}_r$ in satellite body frame, where it is measured with the ST

$$\mathbf{R_m} = \mathbf{CR_r} \tag{8}$$

where $\mathbf{C}$ is the DCM of the rotation from the reference frame to satellite body frame and vectors $\overline{R}_r$ and $\overline{R}_m$ are written in the matrix form as matrix columns.

If the ST is in the tracking mode keeping in its FOV some n detected navigation stars, then it can be assumed that $\mathbf{C}$ is a small-angle matrix that is independent of the rotation order and can be expressed as follows:

$$\mathbf{C} \approx \begin{bmatrix} 1 & \alpha_z & -\alpha_y \\ -\alpha_z & 1 & \alpha_x \\ \alpha_y & -\alpha_x & 1 \end{bmatrix} \tag{9}$$

where $\alpha_x, \alpha_y, \alpha_z$ are small angles of satellite rotation about X, Y, Z axis, respectively. Then subtracting from (8) $\mathbf{R_r}$, the following equation can be written:

$$\delta\mathbf{R} = \delta\mathbf{CR_r} \tag{10}$$

where $\delta\mathbf{R} = \mathbf{R_m} - \mathbf{R_r}$, $\delta\mathbf{C} \approx \begin{bmatrix} 0 & \alpha_z & -\alpha_y \\ -\alpha_z & 0 & \alpha_x \\ \alpha_y & -\alpha_x & 0 \end{bmatrix}$.

Transforming in (10) matrix product and taking into account random measurement errors, this equation can be represented in the following form:

$$\delta\mathbf{R} = \mathbf{R_r}\delta\mathbf{C} + \mathbf{V} \tag{11}$$

where $\delta\mathbf{R} = \begin{bmatrix} \delta R_x \\ \delta R_y \\ \delta R_z \end{bmatrix}$, $\mathbf{R_r} = \begin{bmatrix} 0 & -R_{rz} & R_{ry} \\ R_{rz} & 0 & -R_{rx} \\ -R_{ry} & R_{rx} & 0 \end{bmatrix}$, $\delta\mathbf{C} = \boldsymbol{\alpha} = \begin{bmatrix} \alpha_x \\ \alpha_y \\ \alpha_z \end{bmatrix}$, $\mathbf{V} = \begin{bmatrix} V_x \\ V_y \\ V_z \end{bmatrix}$,

V is random measurement error vector (considered as the white Gaussian noise, having covariance matrix $\mathbf{R} = r\mathbf{I}$).

Then this equation can be considered as a "standard" linear algebraic equation:

$$\mathbf{z_i} = \mathbf{h_i}\mathbf{x} + \mathbf{V_i}$$

$$i = 1, 2, ..n - \text{number of measured vectors} \tag{12}$$

where, $\mathbf{z_i} = \delta\mathbf{R_i}$, $\mathbf{h_i} = \mathbf{R_{ri}} = \begin{bmatrix} 0 & -R_{rz} & R_{ry} \\ R_{rz} & 0 & -R_{rx} \\ -R_{ry} & R_{rx} & 0 \end{bmatrix}_i$, $\mathbf{V_i} = \begin{bmatrix} V_x \\ V_y \\ V_z \end{bmatrix}_i$ $\mathbf{x} = \delta\mathbf{C} = \boldsymbol{\alpha} = \begin{bmatrix} \alpha_x \\ \alpha_y \\ \alpha_z \end{bmatrix}$.

If $n = 1$, only a single vector is measured, then $\det\mathbf{h_i} = -R_{rx}R_{ry}R_{rz} + R_{rx}R_{ry}R_{rz} \equiv 0$, and thus, determining all three angles of satellite attitude is impossible. If it takes informational redundancy, then optimal estimate (providing minimum of standard deviation of satellite attitude errors) can be found with the following LSM formula [13]:

$$\hat{\boldsymbol{\alpha}} = \mathbf{Kz} \tag{13}$$

where $K = \left(H^T R^{-1} H\right)^{-1} H^T R^{-1} H$, $H = [h_1\, h_2\, h_3..h_n]^T$.

3.2.1.2.3 Determination of the angular rate

Direct measurement

Satellite angular rate $\overline{\omega}$ (vector absolute angular velocity) can be measured directly by three-axis rate sensor (RS) that could have mechanical, optical, or microelectromechanical systems (MEMS) design [21, 22] (**Figure 14**). Traditionally, independent of the design type, these RS are usually named "gyros," paying respect to their historical appearance for aerospace vehicle control purposes as a mechanical gyroscope (**Figure 15**).

Measured angular velocity vector $\overline{\omega}$ can be used to determine satellite attitude by the integration of matrix kinematic Poisson's Equation [9, 10]:

$$\dot{\mathbf{C}} = \breve{\omega}\mathbf{C}, \mathbf{C(0)} = \mathbf{C_0} \tag{14}$$
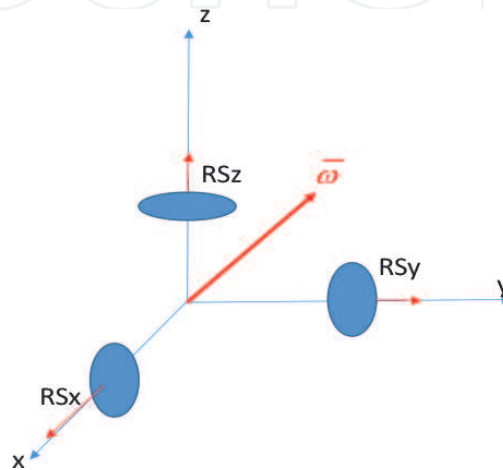
Figure 14.
Measurement of satellite angular velocity $\overline{\omega}$ with three rate sensors RS_x, RS_y, RS_z.

Figure 15.
$\overline{\omega}$-vector sensor RS, BEI QRS-11 single-axis body rate sensor, accuracy, $7\deg/h = 0.0019\deg/s$ (2σ).

where $C = C_{ib}$ $\mathbf{C} = \mathbf{C_{ib}}$ is the DCM between the inertial frame ECI and satellite body frame and $\breve{\omega} = \begin{bmatrix} 0 & \omega_z & -\omega_y \\ -\omega_z & 0 & \omega_x \\ \omega_y & -\omega_x & 0 \end{bmatrix}$ is skew symmetric matrix measured in the satellite frame components of vector of satellite absolute angular velocity. After determination of the DCM, satellite attitude in three Euler angles can be derived with Eq. (7) above. Unfortunately, gyro drift causes unlimited growing up errors in integrated attitude that require periodic corrections from two VMD, measuring the attitude directly (**Figures 10–12**).

Body rate estimator

Often, specifically for attitude stabilization (keeping or aka pointing) mode, satellite angular rate is estimated by using the so-called body rate estimator and is not measured directly by the RS. Indeed, using for attitude keeping mode small angles and linear approximation, we can simplify satellite attitude dynamics model [9] to three single-axis state equations and present it with the stochastic influences as follows:

$$\begin{cases} \dot{\boldsymbol{\omega}} = \mathbf{w} \\ \dot{\boldsymbol{\alpha}} = \boldsymbol{\omega} \\ \mathbf{z} = \boldsymbol{\alpha} + \mathbf{v} \end{cases} \tag{15}$$

where $\boldsymbol{\omega}$ is the angular velocity, $\boldsymbol{\alpha}$ is the satellite deviation angle from the desired direction and $\mathbf{z}$ is the satellite deviation angle measurement with random Gaussian white noise error $\mathbf{v}$. Realistically, it is a wide spectrum correlated process that components have spectral density $r_i = 2\sigma_{v_i}^2 T_{v_i}, i = x, y, z$ (σ_{v_i} is standard deviation of the random error v_i, T_{v_i} is $v_i(t)$ correlation time), w_i is exciting angular acceleration noise with spectral density $q_i = 2\sigma_{wi}^2 T_{wi}$ (σ_{w_i} is standard deviation of the random angular acceleration $w_i = \frac{M_i}{J_i}$, M_i is exciting external random torque, J_i is satellite moment of inertia, T_{w_i} is $w_i(t)$ correlation time).

The linear KF can be applied to synthesize the estimator for the optimal estimation of the vector angle $\boldsymbol{\alpha}$ and the vector of angular velocity $\boldsymbol{\omega}$, using noisy measurements $\mathbf{z}$ [9]:

$$\begin{cases} \dot{\hat{\boldsymbol{\omega}}} = \mathbf{k_{12}}(\mathbf{z} - \hat{\boldsymbol{\alpha}}) \\ \dot{\hat{\boldsymbol{\alpha}}} = \hat{\boldsymbol{\omega}} + \mathbf{k_{22}}(\mathbf{z} - \hat{\boldsymbol{\alpha}}) \end{cases} \tag{16}$$

where $\hat{\boldsymbol{\alpha}}$ and $\hat{\boldsymbol{\omega}}$ are the optimal estimates of the angle $\boldsymbol{\alpha}$ and the angular velocity $\boldsymbol{\omega}$ correspondingly.

Matrix KF (16) is separated in three independent scalar channels for X, Y, Z axis. Its weight coefficients $\mathbf{k_{12}}$ and $\mathbf{k_{22}}$ can be determined by solving KF Riccati Equation [13–15] for each of these three separate channels independently.

It can be shown that in the considering case, the steady-state ($t \to \infty$) KF coefficients are determined by the following formulas (identically for X, Y, Z axes, i = 1,2,3):

$$\begin{cases} k_{12_i} = \sqrt{\xi_i} \\ k_{22_i} = \sqrt{2\xi_i\sqrt{\xi_i}} \end{cases} \tag{17}$$

where $\xi_i = \frac{q_i}{r_i}$ is the ratio of spectral densities of satellite disturbing torque noise to measured attitude error noise (assuming that both are white Gaussian noises). This parameter can be considered as the *filterability index*. Eq. (16) can be represented in the transfer function (Laplace operator) form as a second-order differential equation unit:

$$\begin{cases} \hat{\omega}_i = \dfrac{s}{T_i^2 s^2 + 2d_i T_i s + 1} z_i \\[4mm] \hat{\alpha} = \dfrac{2dT_i s + 1}{T_i^2 s^2 + 2d_i T_i s + 1} z_i \end{cases} \tag{18}$$

where s is the Laplace operator, T_i is the time constant, and d_i is the specific damping coefficient that is determined by the following formulas:

$$\begin{cases} T_i = \dfrac{1}{\sqrt{k_{12_i}}} = \dfrac{1}{\sqrt[4]{\xi_i}} \\[4mm] d_i = \dfrac{k_{22_i}}{2\sqrt{k_{12i}}} = \dfrac{\sqrt{2}}{2} = 0.707 \end{cases} \tag{19}$$

or in other words, the time constant is in inverse proportionality to the filterability index (in ¼ degree) and the specific damping coefficient is conventional for such a second-order unit 0.707 for each of the three channels.

3.2.1.2.4 Multisensory sensor unit (MSU)

As it can be seen from the consideration above, the use of directly measuring devices (e.g., ST and RS) for attitude and body rate determination has a disadvantage. The random noises are at the devices output, and they have to be filtered in the closed control loop of satellite attitude control that puts some constraints to choose the control law coefficients. However, using indirect body rate measurement, the state estimator (filter) unavoidably introduces additional phase delay in the control loop because of the consecutive inclusion of this filter in the control loop. To use the RS (gyro) and the integrator for body rate and attitude determination autonomously for a long time is not possible because of the accumulated attitude errors caused by the integration of the gyro drift. The following scheme (that is common in Aviation) can be considered as free from the disadvantages above. Let us assume that satellite attitude is determined in two ways: continuous integration of RS angular velocity (IMU) and using VMD, for example, ST. Then this ST is used to correct the attitude derived by the integration of RS output. The idea of MSU is shown in **Figure 16**.
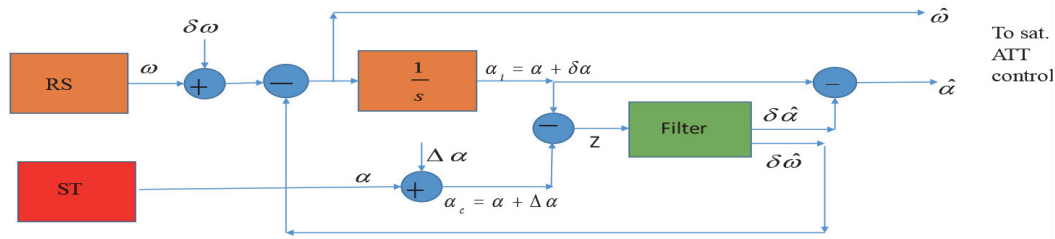
Figure 16.
Integration of multisensory sensor unit (MSU) single-axis channel.

In integrated IMU attitude (IMU = RS + integrator) as in **Figure 14** above (three identical channels), α_i (inertial angle) has been growing with time deterministic error $\delta\alpha$ due to the integration of RS bias $\delta\omega$ and ST has random noisy error $\Delta\alpha\Delta\alpha$. The difference of these signals is equal to the difference of system errors $z = \delta\alpha - \Delta\alpha$. This difference is used for estimation of errors of IMU with a kind of filter, and after the compensation at the system output, the estimates ($\hat{\alpha}$ and $\hat{\omega}$) can be used for satellite control. As it can be seen, in this scheme the filter is not connected in the control loop, and consequently, it does not introduce additional phase delay; however, the scheme still performs its job to filter the noise and estimate RS bias. This scheme can be very effective in practice. It can be presented similar to Eqs. (15) and (16) as follows:

$$\text{IMU model equations :} \begin{cases} \delta\dot{\omega} = w_1 \\ \delta\dot{\alpha} = \delta\omega \\ z = \delta\alpha + \Delta\alpha \end{cases} \tag{20}$$

where $\delta\omega$ is the RS error of measuring the angular velocity; $\delta\alpha$ is attitude error after the integration of the RS signal; z is IMU attitude error measurement with random Gaussian white noise error v $\Delta\alpha = v$, having spectral density $r_1 = 2\sigma_{\Delta\alpha}^2 T_{\Delta\alpha}$ ($\sigma_{\Delta\alpha}$ is the standard deviation of the random error $\Delta\alpha$, $T_{\Delta\alpha}$ is its correlation time); and w_1 is the exciting noise of RS random drift with spectral density $q_1 = 2\sigma_{w1}^2 T_{w1}$ (σ_{w1} is the standard deviation of the random drift, T_w is the $w(t)$ correlation time).

$$\text{KF equations :} \begin{cases} \delta\hat{\dot{\omega}} = k_{12}(z - \delta\hat{\alpha}) \\ \delta\hat{\dot{\alpha}} = \delta\hat{\omega} + k_{22}(z - \delta\hat{\alpha}) \end{cases} \tag{21}$$

where KF coefficients k_{12} and k_{22} are determined by (17), substituting there q_1 and r_1 instead of q and r.

3.2.2 Actuators

3.2.2.1 Propulsion system (PS)

Satellite propulsion system [9, 10] is usually designed for satellite orbital and/or angular control. In the first case, PS is commanded from the ground OC by TLM commands in some cases when satellite orbit has to be changed (orbit correction, deorbiting, collision avoidance), in the second controlled automatically from onboard AODCS. It consists of such typical elements as orbital and attitude thrusters (number and installation scheme depending on certain application), propulsion tank with associated pipes, valves, regulators, and electronics. General principles of PS act independently of the type (ion thrusters (0.01–0.1 N), liquid propellant and solid motor (100–10,000 N), cold gas (1-3 N)).
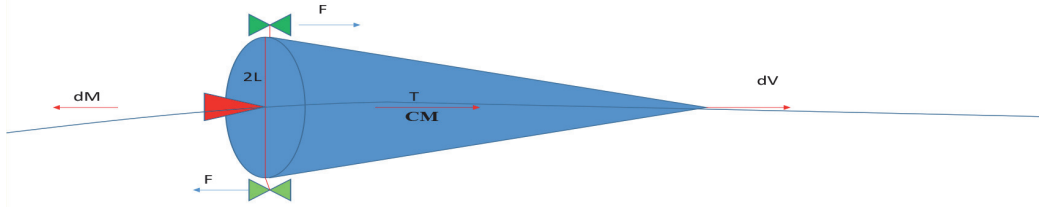
Figure 17.
Satellite control with PS thruster principles.

Figure 15 illustrates the satellite control with PS thruster principles. The principle of the formation of the propulsion jet force can be presented by the following equation of variable mass body dynamics that from Russian sources, for example, [23], is known as Prof. I. Meshchersky's equation:

$$M\frac{dV}{dt} = F - V_p\frac{dm}{dt} \tag{22}$$

where M is the mass body, F is the external force, V_P is the propellant exhaust velocity and m is the propellant mass. The term $-V_p\frac{dm}{dt}$ is the propulsion force (propulsion thrust) (**Figure 17**).

$$T = -V_p\frac{dm}{dt} \tag{23}$$

In Section 3.2.2.1.2, it is always $\frac{dm}{dt} < 0$, then $T > 0$. Usually for any propulsion system, let us introduce parameter *specific pulse I_{sp}*, where $I_{sp} = \frac{T}{g|\dot{m}|} = \frac{V_p}{g}$ then $V_p = I_{sp}g\dot{m}$ and $T = -I_{sp}g\dot{m}$. If the satellite thruster is installed such as satellite point of the center of mass (CM) is located on the line of the action of the force T (red thruster in **Figure 17**), then the thruster can serve for satellite orbit correction, and the pulse of the control thrust causes increment of satellite velocity $dV = \frac{1}{M}Tdt$. If satellite thrusters are installed in such a way that having an arm L from the CM, then they create rotating torque (green reversible thruster pair in **Figure 17**) and can be used for attitude control (control torque is $T_r = LT$). And the increment in attitude angle for the time dt of the pair of thruster activation will be $d\alpha = \frac{T_r}{J}dt$.

The expelled propulsion mass Δm can be calculated with the K. Tsiolkovsky formula [9, 24] that follows from Eq. (22)

$$\Delta m = m_0\left[1 - e^{-\frac{dV}{gI_{sp}}}\right] \tag{24}$$

where m_0 is the propellant initial mass. Photos of I. Meshchersky and K. Tsiolkovsky are presented (**Figures 18** and **19**).

Discrete pulse modulation control is usually used to minimize the consumption of the propellant for attitude control [9]. Examples of the gas thruster and the tank are presented in **Figures 20** and **21**.

3.2.2.2 Magnetic torque rods (MTR)

Magnetorquers are essentially sets of electromagnets. A conductive wire is wrapped around a ferromagnetic core which is magnetized when excited by the electric current caused by the control voltage applied to the coil. The disadvantage of this design is the presence of a residual magnetic dipole that remains even when

Figure 18.
Prof. I. Meshchersky (1859–1935).

Figure 19.
K. Tsiolkovsky (1857–1935).

Figure 20.
Cold gas GN-2 thruster, nominal thrust 3.6 N (230 psi), specific impulse 57 s.

the coil is turned off because of the hysteresis in the magnetization curve of the core. It is therefore necessary to demagnetize the core with a proper demagnetizing procedure. Normally, the presence of the core (generally consisting of ferromagnetic) increases the mass of the system. The control voltage is controlled by AODCS control output (**Figures 18–20**). The magnetic dipole generated by the magnetorquer is expressed by the formula:

$$\overline{M} = ni\overline{S} \qquad (25)$$

Figure 21.
60 liter propulsion gas tank.

where n is the number of turns of the wire, i is the current provided, and $\overline{S}$ is the vector aria of the coil. The dipole interacts with the Earth magnetic field, generating a torque whose expression is:

$$\overline{T}_m = \overline{M} \times \overline{B} \tag{26}$$

where $\overline{M}$ is the magnetic dipole vector moment, $\overline{B}$ is the Earth magnetic field induction vector and $\overline{T}_m$ is the generated magnetic torque vector. This equation in the scalar form is as follows:

$$\begin{bmatrix} T_{mx} \\ T_{my} \\ T_{mz} \end{bmatrix} = \begin{bmatrix} 0 & B_z & -B_y \\ -B_z & 0 & B_x \\ B_y & -B_x & 0 \end{bmatrix} \begin{bmatrix} M_x \\ M_y \\ M_z \end{bmatrix} \tag{27}$$

Typically, three coils are used; the three-coil assembly usually takes the form of three perpendicular coils, because this setup equalizes the rotational symmetry of the fields which can be generated; no matter how the external field and the craft are placed with respect to each other, approximately the same torque can always be generated simply by using different amounts of current on the three different coils (**Figure 22**).

It can be seen from Eq. (26) that MTR cannot generate the magnetic torque in the direction that is parallel to Earth magnetic field $\overline{B}$ ($\overline{M}\|\overline{B}$) and it always is perpendicular to the Earth magnetic field vector $\overline{T}_m \perp \overline{B}$. Unfortunately, from Eq. (27), the required magnetic moments cannot be found, because it has zero determinant, and we cannot invert it.

$$\Delta = \begin{vmatrix} 0 & B_z & -B_y \\ -B_z & 0 & B_x \\ B_y & -B_x & 0 \end{vmatrix} = -B_x B_y B_z + B_x B_y B_z = 0 \tag{28}$$

However, the following approach can be used to find required vector $\overline{M}$ [9]. When we take cross-product of $\overline{B}$ with both sides of Eq. (26) and take into account that it is useless to apply $\overline{M}$ in parallel direction to $\overline{B}$, and hence we can require that $\overline{M} \perp \overline{B}$ and $\overline{M} \cdot \overline{B} = 0$, then the following formula can be derived:
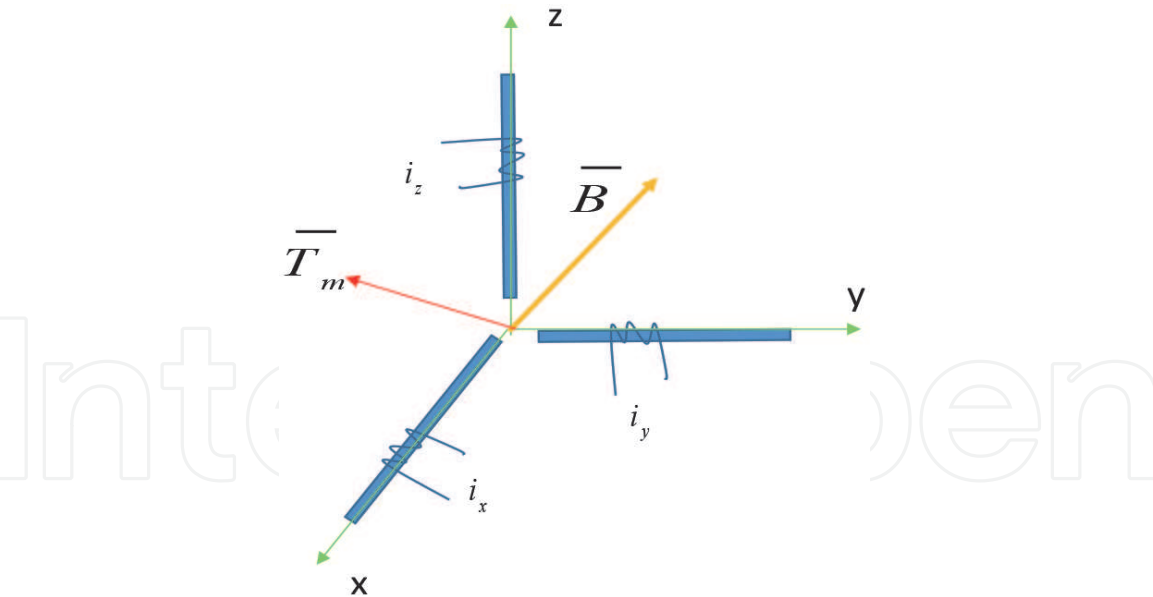
Figure 22.
3D orthogonal magnetic torque rods.

$$\overline{M} = \frac{\overline{B} \times \overline{T}_m}{B^2} \tag{29}$$

Another MTR control method is the so-called B-dot control [25].

$$\overline{M} = -k\overline{B} \tag{30}$$

where k is control gate coefficient.

As the result of (29) control, the satellite will reduce its body rate and is finally slow rotated along Earth's geomagnetic field line (vector $\overline{B}$). Eventually it achieves its threshold of capture by the gravity gradient effect.

If the redundancy is required, it is provided by additional (redundant) coil with the same core (**Figure 23**).

Figure 23.
Magnetic torque rod SSTL MTR-30, magnetic moment, $M = 30$ Am^2.

3.2.2.3 Reaction/reaction-momentum wheels (RW/RMW)

Reaction wheels (RW), aka momentum exchange devices [9] or reaction-momentum wheels (RMW), have massive rotated rotor with big axial moment of inertia with respect to the axis of rotation. They are electrically controlled by the electric motors and the rotor is installed on the rotating motor shaft. The controlled voltage, applied to the control winding of the motor, controls its rotor angular speed. The product of the rotor angular acceleration $\dot{\Omega}$ multiplied by its axial inertia $\mathbf{I}$ is the RW generated inertia control torque $\mathbf{T_i} = \mathbf{I}\dot{\Omega}$ that is applied to the satellite body in opposite to the acceleration direction. Special embedded angular speed
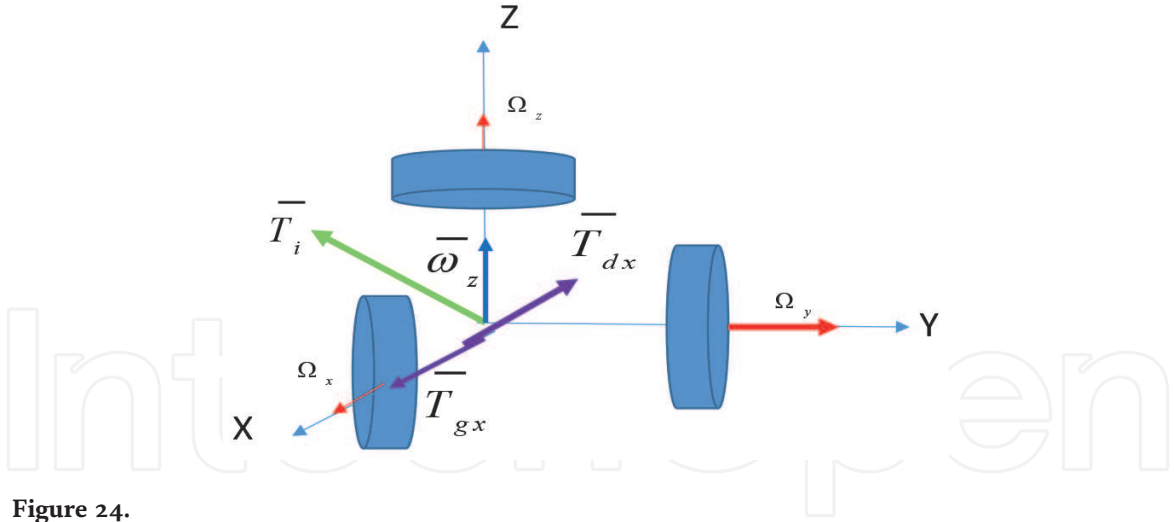
Figure 24.
Three orthogonal reaction wheels (RW).

sensor (tachometer) measures the motor rotor angular speed and allows organizing RW inertia torque control proportional to the applied control voltage. At least three RW, as in **Figure 24**, are required to produce control torque vector in three-dimensional spatial, having desired value and pointed in the desired direction. Sometimes redundant unit of three redundant wheels or one with 4th redundant skewed wheel is applied to meet reliability requirements.

RW can generate control inertia torques $\mathbf{T_i}$ only when they are accelerated or decelerated. With this torque, they cannot compensate a permanent disturbance torque $\mathbf{T_d} = \mathbf{const}$ applied to satellite for a long enough time and come eventually to some maximum/minimum available speed aka *the saturation speed*. At that state $\overline{T}_i$ becomes zero. That is why RW is usually applied with other types of actuators such as MTRs or gas thrusters to de-saturate the RW to use them as the source of $\mathbf{T_i}$ again.

In general case, RW can be run around in some nominal angular speed $\mathbf{\Omega_0}$. In this case they can be named as reaction-momentum wheel (RMW) and then just RW. Mathematically RW/RMW dynamics can be presented as follows. Let us consider satellite with RW unit angular momentum:

$$\mathbf{H_s} = \mathbf{H} + \mathbf{h} \tag{31}$$

where $\mathbf{H} = \mathbf{J\omega}$ is the satellite *absolute* angular momentum vector (column matrix), $\mathbf{\omega}$ is the vector of satellite absolute angular velocity, $\mathbf{J} = \begin{bmatrix} J_{xx} & -J_{xy} & -J_{xz} \\ -J_{yx} & J_{yy} & -J_{yz} \\ -J_{zx} & -J_{zy} & J_{zz} \end{bmatrix}$ is the satellite inertia matrix, $\mathbf{h} = \mathbf{I\Omega}$ is the RMW *relative* angular momentum vector, $\mathbf{\Omega}$ is the RW relative rotation speed vector, and $\mathbf{I} = \begin{bmatrix} I_{xx} & 0 & 0 \\ 0 & I_{yy} & 0 \\ 0 & 0 & I_{zz} \end{bmatrix}$ is the RW inertia matrix.

Then differentiating (31) in rotating with angular velocity satellite axis $\mathbf{\omega}$ and using Euler's rigid body dynamics formula [9], we can get the following equation:

$$\dot{\mathbf{H}} + \breve{\omega}\mathbf{H} = -\dot{\mathbf{h}} - \breve{\omega}\mathbf{h} + \mathbf{T} \tag{32}$$

where $\breve{\omega} = \begin{bmatrix} 0 & -\omega_z & \omega_y \\ \omega_z & 0 & -\omega_x \\ -\omega_y & \omega_x & 0 \end{bmatrix}$ is the satellite angular velocity matrix and $\mathbf{T}$ is the vector of the external torque applied to the satellite. In the right side of Eq. (32),

we can see two terms that have meaning of torques applied from the RMW unit to the satellite body: $-\dot{\mathbf{h}} = \mathbf{T_i}$ the inertial torque and $-\breve{\boldsymbol{\omega}}\mathbf{h} = \mathbf{T_g}$ the gyro torque. They are RMW generated torques that can be used for the satellite attitude control. Eq. (32) presents satellite attitude dynamics under the action of RMW torques. The RW dynamics can be presented similar to Eq. (32):

$$\dot{\mathbf{h}}_{\mathbf{w}} + \breve{\boldsymbol{\omega}}\mathbf{h}_{\mathbf{w}} = \mathbf{M_w} + \mathbf{M_f} \tag{33}$$

where $\mathbf{h_w} = \mathbf{h} + \mathbf{h_c}$ is the absolute RW momentum, $\mathbf{h_c} = \mathbf{I}\boldsymbol{\omega}$ is the carrier component of RW absolute momentum, **QUOTE** $\mathbf{M_w}$ is the RW motor control torque, and $\mathbf{M_f}$ is the RW friction torque.

Eq. (33) can be represented in the following form:

$$\dot{\mathbf{h}} = \mathbf{I}\dot{\boldsymbol{\Omega}} = -\mathbf{I}\dot{\boldsymbol{\omega}} - \breve{\boldsymbol{\omega}}(\mathbf{h} + \mathbf{h_c}) + \mathbf{M_w} + \mathbf{M_f} \tag{34}$$

where $\mathbf{M_f} = -\mathbf{k_e}\boldsymbol{\Omega} - \mathbf{M_{df}}\,\text{sgn}\,\boldsymbol{\Omega}$ is the friction torque, $\mathbf{k_e}$ is the motor natural damping coefficient, $\mathbf{M_{df}}$ is the dry friction torque, and $\mathbf{M_w}$ is the control motor torque.

The torque $\mathbf{M_f}$ usually consists of two components: the viscous torque (counter electromotive voltage in the control coil) $-\mathbf{k_e}\boldsymbol{\Omega}$ and dry or Coulomb friction torque in the RMW bearings—$\mathbf{M_{df}}\,\text{sgn}\,\boldsymbol{\Omega}$. The control torque $\mathbf{M_w}$ can be set as follows:

$$\mathbf{M_w} = -(\mathbf{k_\Omega} + \mathbf{k_e})(\boldsymbol{\Omega} - \boldsymbol{\Omega_0}) - \mathbf{k_T}\mathbf{T_c} \tag{35}$$

where $\mathbf{k_\Omega}$ is the motor control damping coefficient, $\boldsymbol{\Omega_0}$ is the desired angular RMW speed, $\mathbf{k_T}$ is the control torque coefficient, and $\mathbf{T_c}$ is requested from AODCS OBC control torque. Taking into account Eq. (35), Eq. (34) can be rewritten in the following form:

$$\mathbf{I}\dot{\boldsymbol{\Omega}} + (\mathbf{k_\Omega} + \mathbf{k_e})\boldsymbol{\Omega} = (\mathbf{k_\Omega} + \mathbf{k_e})\boldsymbol{\Omega_0} + \mathbf{T_c} - \mathbf{I}\dot{\boldsymbol{\omega}} - \breve{\boldsymbol{\omega}}(\mathbf{h} + \mathbf{h_c}) + \mathbf{M_f} \tag{36}$$

In the operator Laplace s-form (transfer function), Eq. (36) can be rewritten as follows:

$$\boldsymbol{\Omega}(s) = \mathbf{W}(s)\left\{\boldsymbol{\Omega_0} + \mathbf{k}_w^{-1}\left[\mathbf{T_c} - \mathbf{I}s\boldsymbol{\omega} - \breve{\boldsymbol{\omega}}(\mathbf{h} + \mathbf{h_c}) + \mathbf{M_f}\right]\right\} \tag{37}$$

where $\mathbf{W}(s) = \begin{bmatrix} (T_{wx} + 1)^{-1} & 0 & 0 \\ 0 & (T_{wy} + 1)^{-1} & 0 \\ 0 & 0 & (T_{wz} + 1)^{-1} \end{bmatrix}$ is the RW matrix

transfer function, $T_{w_x} = \frac{I_x}{k_{\Omega x} + k_{ex}}$, $T_{w_y} = \frac{I_x}{k_{\Omega y} + k_{ey}}$, $T_{w_x} = \frac{I_x}{k_{\Omega z} + k_{ez}}$ is the RW time constants, and.

$$\mathbf{k}_w = \begin{bmatrix} (k_{\Omega x} + k_{ex})^{-1} & 0 & 0 \\ 0 & (k_{\Omega y} + k_{ey})^{-1} & 0 \\ 0 & 0 & (k_{\Omega z} + k_{ez})^{-1} \end{bmatrix}$$ is the RW control speed

coefficient.

It should be noted that sometimes the RW control loop is more sophisticated. Special integrators could be connected into the loop to memorize and compensate the dry friction torques acting in bearings. Some small nominal rotating speed can be set for all three RMW to eliminate the dry friction torque having a pike when the wheel speed is zero $\boldsymbol{\Omega} = \mathbf{0}$.

However, more representative case is when $\boldsymbol{\Omega_0}$ is set (usually in one direction as in **Figure 23**—axis Y) to provide to the satellite a gyro-stiffness (gyro-stabilization capability) with respect to another two axes X and Z.

Indeed, if we put in (32) that $\dot{\omega}_x = \dot{\omega}_y = \dot{\omega}_z = \dot{\Omega}_x = \dot{\Omega}_y = \dot{\Omega}_z = 0$, and $\omega_x = \omega_z = \Omega_x = \dot{\Omega}_y = \dot{\Omega}_z = 0$, $\omega_y = \omega_0 = const, \Omega_y = \Omega_0 = const$, then it can be written as:

$$\begin{cases} -\omega_z\left(H_y + h_y\right) = T_x \\ \omega_x\left(H_y + h_y\right) = T_z \end{cases} \tag{38}$$

where $H_y = J_y\omega_0, h_y = I_y\Omega_0$. In this case carrier orbital angular velocity ω_0 helps to increase satellite momentum $H_{sy} = H_y + h_y$. Eq. (38) is known as three degrees of freedom of a free gyroscope precession [21] and represents the gyro-stabilization effect: that gyroscope vector H_{sy} being free of disturbing torques can keep its direction and value in inertial spatial (**Figure 25**).

Figure 25.
Reaction/momentum wheel HR-0610, torque, $75 \cdot 10^{-3}$Nm; momentum, $(4 - 12)$ Nms.

3.2.3 AODCS OBCS

Independently of sytem arhitecture; it is separate dedicated to AODCS computer, or a special AODCS card within central satellite C&DH computer, it is the integration element of AODCS [1, 11]. AODCS system may consist of the computer (computer card) itself (OBC) and auxiliary intercommunication electronic units (electronic cards) AEU carrying DC/DC electric power conversion and I/O (analog and digital) interface and commutation functions.

OBC can be divided into two parts: the hardware (HW, power convertor, processor, input/output [I/O] convertors, non-volatile and volatile memory) and the software (SW, operation system [OS] and vital or functional software [VS/FS]) (**Figure 26**).

What makes the satellite OBC essentially different for the airplane OBC is that its SW can be uploaded and updated from the ground and during operation and scheduled maintenance. OS OBC includes generic computer programs: program of I/O interface, time schedule (dispatcher), embedded test, timer and standard mathematic functions. Satellite SW often is considered as satellite *SW subsystem* that is verified during development (with mathematical high-fidelity Matlab/Simulink simulators and semi-natural processor-in-the-loop (PIL) simulators). SW subsystem should be tested to meet SW requirements [26, 27]. The flight version of the SW subsystem is supported with operation real-time satellite simulators (RSS) [1, 11] located in operation center. It should be mentioned that only final AODCS
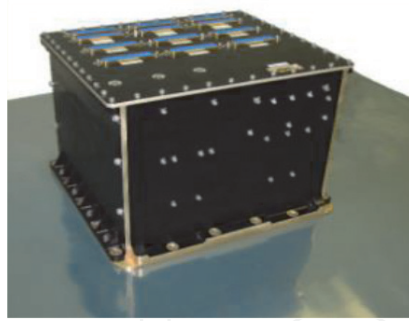
Figure 26.
Satellite OBCS, MAC-200 (C&DH unit with AODCS card) comprises of two OBC: Prime and redundant (cold reserve).

(OBC (HW + SW), sensors, and actuators) *functional test* [2] that should be performed in the Space Qualification Laboratory [7] during satellite Space Qualification and Acceptance campaign can really minimize the risk of launching a not ready satellite and prevent against AODCS refinishing in orbit during commissioning and operation.

VS can be separated in two parts, ODCS SW and ADCS SW. For both parts, I/O interface with sensors and actuators is determined in special interface control document(s) (ICD), describing type, certain connectors, and electrical parameters of the exchanging data. These data before using them for functional tasks are pre-processed in OBC with special algorithms.

3.2.3.1 Satellite sensors/actuators data preprocessing

This group of algorithms performs the following common tasks:

- Convert data into required physical parameters and units, taking into account certain sensor input–output scale function.

- Transform data in certain device frame and compensate device misalignment, bias and scale function errors if it is possible, monitor device state, establishing "on/off," "work/control," "data bad/good" flags.

- Transfer to C&DH TLM data about sensor/actuator state and their data.

- Perform some other auxiliary functions if they are required.

- Main functional tasks ODCS SW and ADCS SW can be listed as below.

3.2.3.2 ODCS SW

3.2.3.2.1 Satellite orbit propagation (OP)

To understand the idea of propagation of satellite orbit in Earth gravity field to the simplest, Keplerian motion propagator based on spherical Earth gravity field model might be used [9]; however more realistic results can be obtained with more accurate propagator, taking into account the second zonal harmonic J_2 in the function of approximation of Earth gravitational potential. The following equations of motion of satellite center of mass in Earth gravitational field can be considered [9]:

$$\ddot{x} = -\mu\frac{x}{r^3} + A_{J2}\left(15\frac{xz^2}{r^7} - 3\frac{x}{r^5}\right),$$

$$\ddot{y} = -\mu\frac{y}{r^3} + A_{J2}\left(15\frac{yz^2}{r^7} - 3\frac{y}{r^5}\right),$$

$$\ddot{z} = -\mu\frac{z}{r^3} + A_{J2}\left(15\frac{z^3}{r^7} - 9\frac{z}{r^5}\right),$$

$$r = \sqrt{x^2 + y^2 + z^2},$$

(39)

where x, y, z are the Cartesian coordinates of satellite center of mass in inertial frame ECI, $r = \sqrt{x^2 + y^2 + z^2}$ is the module of the radius vector from the center of Earth to satellite center of mass, $\mu = 3.986004418 \cdot 10^{14}$ $[m^3/s^2]$ is the Earth gravitational constant, $A_{J2} = \frac{1}{2}J_2 \cdot R_e^2$ is a constant, $J_2 = 0.00108263$ is the second zonal harmonic coefficient in the raw of Earth potential function, and $R_e = 6378137.00$ m is the mean radius of the Earth at the equator.

These equations can propagate satellite position and velocity (x, y, z and $\dot{x}, \dot{y}, \dot{z}$) in the inertial Cartesian ECI coordinate system if the initial parameters are initially set $x_0 = x(0), y_0 = y(0), z_0 = z(0)$ and $\dot{x}_0 = \dot{x}(0), \dot{y}_0 = \dot{y}(0), \dot{z}_0 = \dot{z}(0)$. They can be periodically determined from GPS or MCC TLM information. The propagation credibility time depends on orbit perturbations [9, 10, 27] and required accuracy. The most accurate and common ground propagators are NORAD Simplified Perturbation Model (SGP) propagators. NORAD SGP is used for proving to users two-line element (TLE) satellite orbital data. For the low Earth orbit (LEO), having altitude below 6000 km (period about 225 min), they provide position accuracy about 1 km within a few days that for many users is accurate enough and needs to be updated once or twice per week. Currently almost every satellite is equipped with GPS and its onboard propagators are practically continuously corrected with GPS (and sometimes MCC TLM) data that provide position within 10–100 m and velocity within 0.01–0.1 m/s accuracy range. Only some short periods of GPS data outage require orbit propagation. In addition to satellite position and velocity, OP calculates conventional orbital parameters (**Figure 14**) that can be computed with the following formulas [9]:

$$a = \frac{\mu}{2\left[\dfrac{\mu}{r} - \dfrac{V^2}{2}\right]}$$

$$i = \cos^{-1}\frac{h_{zi}}{h}$$

$$\Omega = \tan^{-1}\frac{h_{xi}}{-h_{yi}}$$

$$\nu = \tan^{-1}\frac{\overline{r} \cdot \overline{V}}{p - r}$$

$$u = \sin^{-1}\frac{z_i}{r\sin i}$$

$$\omega = u\text{-}\theta$$

(40)

where $\overline{h} = \overline{r} \times \overline{V}$ is the satellite orbital linear momentum vector, a is the satellite orbit semi-major axis, $h = \sqrt{h_{xi}^2 + h_{yi}^2 + h_{zi}^2}$ is the linear momentum module, $p = a(1\text{-}e^2)$ is the satellite orbit focal parameter, i is the satellite orbit inclination angle, Ω

is the satellite orbit right ascension of ascending node angle (RAAN), u is the argument of latitude angle, ν is the satellite true anomaly angle, and ω is the satellite orbit argument of perigee angle (**Figure 27**).
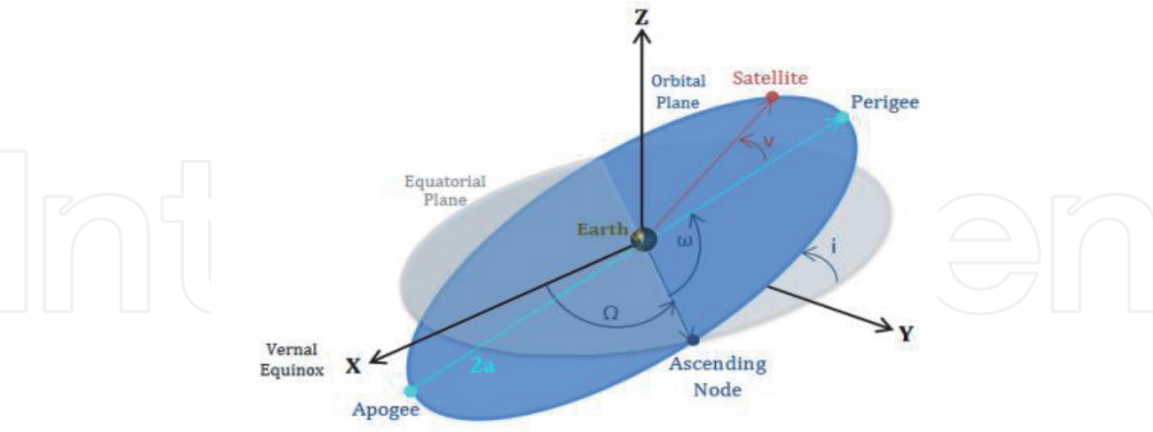
Figure 27.
*Satellite orbit in the inertial ECI (XYZ) coordinate system.*

3.2.3.2.2 Orbital thrusters control

If orbit maneuver is required, then it can be commanded by AODCS SW autonomously, or special control commands TLM (uploaded command tables) are sending to satellite AODCS, and in predetermined time they are executed activating at scheduled time for the calculated period (Δt) the orbital thrusters that provide for the required orbital correction/maneuver pulse($F\Delta t$).

3.2.3.3 ADCS SW

3.2.3.3.1 Satellite attitude and angular velocity estimation algorithms

This group of algorithms was presented above in 3.2.1.2 and can be used here.
For example, let us consider single-axis stabilized satellite that should keep one axis (e.g., Z) permanently pointed to the Sun as in **Figure 28**. Only two angles of the satellite deviation from this direction and their angular velocities are required to know to point and keep it in this direction. The satellite has two-axis Sun sensor that
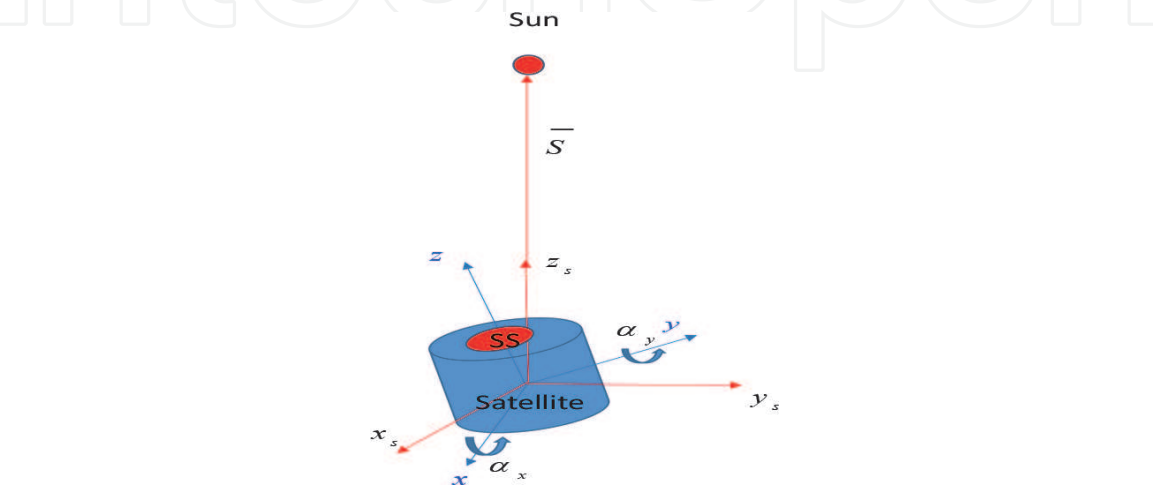
Figure 28.
Satellite pointed by the Z-axis to the sun.

can measure two angles α_x, α_y of satellite deviation from the sun direction. Its axes coincide with the satellite axes xyz. The axis z is the sensitivity axis that nominally should point into the Sun's direction (center of brightness), and xy is the focal plane. The Sun vector is referenced in the Sun frame as $S_r = [0\ 0\ S]^T$ and is measured in the Sun sensor measured frame as $S_m = \begin{bmatrix} S_x & S_y & S_z \end{bmatrix}^T$.

In **Figure 28**, xyz is the satellite body frame, $x_s y_s z_s$ is the Sun reference frame, SS is the two-axis Sun sensor and α_x and α_y are the turn angles of satellite x and y axis accordingly.

The following formula represents the mathematical transformation of the Sun vector from the reference into the body frame:

$$\mathbf{S_m} = \mathbf{C_{bs}} \mathbf{S_r} \tag{41}$$

where $\mathbf{S_r} = [0\ 0\ S]^T$, $\mathbf{S_m} = \begin{bmatrix} S_x & S_y & S_z \end{bmatrix}^T$, and $\mathbf{C_{bs}}$ is the DCM between the reference (Sun) and measured (satellite) frames. Let us consider that the order of rotation from the Sun to the satellite frame is 3-2-1 $(\alpha_z, \alpha_y, \alpha_x)$; the DCM matrix $\mathbf{C_{bs}}$ is as follows [9]:

$$\mathbf{C_{bs}} = \begin{bmatrix} \cos\alpha_y \cos\alpha_z & \cos\alpha_y \sin\alpha_z & -\sin\alpha_y \\ -\cos\alpha_x \sin\alpha_z + \sin\alpha_x \sin\alpha_y \cos\alpha_z & \cos\alpha_x \cos\alpha_z + \sin\alpha_x \sin\alpha_y \sin\alpha_z & \sin\alpha_x \cos\alpha_y \\ \sin\alpha_x \sin\alpha_z + \cos\alpha_x \sin\alpha_y \cos\alpha_z & -\cos\alpha_x \cos\alpha_z + \cos\alpha_x \sin\alpha_y \sin\alpha_z & \cos\alpha_x \cos\alpha_y \end{bmatrix} \tag{42}$$

Then from (41), (42) can derive the following formulas:

$$\begin{cases} S_{xm} = -S\sin\alpha_y \\ S_{ym} = S\sin\alpha_x \cos\alpha_y \\ S_{zm} = S\cos\alpha_x \cos\alpha_y \end{cases} \tag{43}$$

From (43), desired angles and can be derived that can be used for satellite attitude control.

$$\begin{cases} \alpha_x = \tan^{-1} \dfrac{S_{ym}}{S_{zm}} \\ \alpha_y = -\sin^{-1} \dfrac{S_{xm}}{\sqrt{S_{ym}^2 + S_{zm}^2}} \end{cases} \tag{44}$$

3.2.3.3.2 Angular velocities (body rates)

Let us also assume that the satellite does not have angular velocity sensors RS and its angular velocities should be derived from the measured angles α_x and α_y. Simple low-frequency first-order differentiating fitters can be applied for this purpose. Laplace operator s-form (transfer functions) of these filters are presented below:'

$$\begin{cases} \hat{\dot{\alpha}}_x = \dfrac{s}{T_{fx}s + 1} \alpha_x \\ \hat{\dot{\alpha}}_y = \dfrac{s}{T_{fy}s + 1} \alpha_y \end{cases} \tag{45}$$

where T_{fx}, T_{fy} are filter time constants, typically, $T_f < (3 - 10)\ s$.

3.2.3.3.3 Satellite control algorithms

If not the optimization criterion to characterize the control quality [13] is required, then conventional negative feedback closed control loop with linear PID (proportional, integral, and damping) control law [9] that provides a good performance for many practical satellite control applications can be used to satisfy the requirements. They are typical for any automatic control system requirements: such as transfer process decay time and overshooting, residual static error caused by the permanent external disturbance, etc. Today, attitude control system performance can be verified mainly on ground with simulation. If we try to evaluate it in flight, then only onboard attitude sensors TLM data can be used for postprocessing, and it should be taken into account that mainly sensors that detect high-frequency noise (perceived errors) will be observable and low-frequency components (sensor biases) are compensated in the closed control attitude stabilization loop. Simple example of single-axis satellite attitude stabilization control loop is presented below. It is a simplified linear model; however, it presents the stabilization principle and essential features. Let us assume that a simple, positional, and damping control law is used to stabilize satellite axis Z in Sun direction $\overline{S}$ as in the example C1 for attitude and angular rate determination above. Let us assume that only the one-axis control channel X is considered; small angle α_x ($\tan \alpha_x \approx \alpha_x$) is measured with SS (44), and its rate is derived with linear differentiating filter (45). Then requested PD control torque can be presented by the following formula:

$$T_{cx} = -k_{px}\alpha_{xm} - k_{dx}\frac{s}{T_{fx}+1}\alpha_{xm} \tag{46}$$

where k_{px} is the position control coefficient, k_{dx} is the damping control coefficient, $s = \frac{d}{dt}$ is the Laplace operator, T_{fx} is the differentiating filter time constant, $\alpha_{xm} = \alpha_x + \Delta\alpha_x$ is the measured angle α_x, α_x is the true value and $\Delta\alpha_x$ is the measured error. Let us assume that this torque is generated by only one MTR Y. Eq. (27) is determined as:

$$T_{cx} = B_z M_y = B_z k_{TRy} u_y \tag{47}$$

where $B_z = const$ is the local Z component of Earth magnetic induction vector, $M_y = k_{TRy} u_y$ is the Y MTR magnetic moment, k_{TRy} is the Y MTR control gate and i_y is the control voltage applied to Y MTR winding. Then as it follows from (46), (47) requested from the AODCS OBC control voltage to the winding of Y MTR is:

$$u_y = -K_{px}\alpha_{xm} - K_{dx}\frac{s}{T_{fx}+1}\alpha_{xm} \tag{48}$$

where $K_{px} = \frac{k_{px}}{B_z k_{TRy}}$ and $K_{dx} = \frac{k_{dx}}{B_z k_{TRy}}$ are position and damping magnetic control coefficients.

Let us take a ball-shaped satellite with the inertia matrix as follows:

$J = \begin{bmatrix} J_x & 0 & 0 \\ 0 & J_y & 0 \\ 0 & 0 & J_z \end{bmatrix}$ where $J_x = J_y = J_z J_x = J_y = J_z$. Then in inertial spatial, its linear

angular dynamical equations for the axis X can be approximately written as follows:

$$J_x s^2 \alpha_x = T_{c_x} + T_{d_x} \tag{49}$$

where $s = \frac{d}{dt}$ is the Laplace operator, T_{c_x} is the control torque, and T_{d_x} is the disturbing external torque (satellite residual and induction magnetism torque, atmosphere drug torque, solar pressure torque). Then substituting in Eq. (49) Eqs. (47) and (48), we can rewrite it as follows:

$$J_x s^2 \alpha_x = -k_{px}\alpha_{xm} - k_{dx}\frac{s}{T_{fx}s + 1}\alpha_{xm} + T_{dx} \qquad (50)$$

Let us divide all terms in Eq. (50) by the coefficient k_p and substitute α_{xm} value, then it can be represented in the following form:

$$\left(T_x^2 s^2 + 2d_x T_x \frac{s}{T_{fx}s + 1} + 1\right)\alpha_x = \frac{1}{k_{px}}T_{dx} - \Delta\alpha_x \qquad (51)$$

where $T_x = \sqrt{\frac{J_x}{k_{px}}}$ is the X control channel time constant and $d_x = \frac{k_{dx}}{2\sqrt{k_{px}J_x}}$ is the Xcontrol channel-specific damping coefficient. Eq. (51) is a third-order linear differential equation and could be analytically analyzed. In particular its stability can be analyzed with algebraic Hurwitz criterion [13]. However, more simple and general results can be obtained with the following approximate consideration. If $T_{fx} << T_x$, then by the filter time constant, T_{fx} can be neglected, and (51) can approximately be considered as a standard second-order control unit, presented by the second-order linear time invariant (LTI) differential equation and rewritten as follows:

$$\left(T_x^2 s^2 + 2d_x T_x s + 1\right)\alpha_x \simeq \frac{1}{k_{px}}T_{dx} - \Delta\alpha_x \qquad (52)$$

As it follows from Eq. (52), steady-state error in attitude stabilization can be calculated with the formula:

$$\left(T_x^2 s^2 + 2d_x T_x s + 1\right)\alpha_x \simeq \frac{1}{k_{px}}T_{dx} - \Delta\alpha_x \qquad (53)$$

where $T_{dx0} = const$ and $\Delta\alpha_{x0} = const\Delta\alpha_{x0} = const$ (ATT sensor bias).

For Eq. (52), *the optimal* damping coefficient is $d_x = \frac{\sqrt{2}}{2} = 0.707$ [13].

Numerical example

Let us evaluate satellite time constant T_x. Let us assume that for the LEO satellite magnetic field induction vector $\overline{B}$ has the following value of the projection on the Sun direction.

and MTR has the following parameters: maximal magnetic moment $M_{y\,max} = 35 Am^2$, maximal control current $I_{y\,max} = 100$ mA, winding resistance $R = 280$ Ohm; and maximal control voltage $u_{ymax} = R \cdot I_{y\,max} = 28$ V. MTR gate is $k_{TRy} = \frac{M_{y\,max}}{u_{y\,max}} = \frac{35Am^2}{28V} = 1.25 Am^2/V$. Then maximal available magnetic torque is $T_{cx\,max} = 10^{-3}Nm$. If maximal linear zone for this control channel is $\alpha_{y\,max} = \frac{\pi}{2}$ rad, then the position control coefficient k_{px} can be calculated with the following formula:

$$k_{px} = \frac{T_{cx\,max}}{\alpha_{max}} \qquad (54)$$

For the data above, it has the value of $k_{px} = \frac{0.001}{3.14 \cdot 0.5} = 6.366 \cdot 10^{-4}$ Nm/rad. Let us consider example of the first Soviet satellite "Sputnik" (SS-1) that had the

mass $m = 83.6$ kg and the radius $R = 0.29$ m and take the assumption that its mass was homogeneously distributed within its spherical volume of $V = \frac{4}{3}\pi R^3 = 0.1$ m³, and then its inertia ($J = J_x = J_y = J_z$) can be calculated with the following formula:

$$J = \frac{2}{5}mR^2 \tag{55}$$

as for a homogeneous sphere. Substituting into Eq. (55) the data above, we can calculate that for SS-1 $J = 2.82$ kgm², then its time constant with the considered MTR control might be:

$$T_x = \sqrt{\frac{J_x}{k_{px}}} = \sqrt{\frac{2.82 kgm^2}{6.366 \cdot 10^{-4} kgm^2 s^{-2}}} = 66.56 \text{ s.}$$

Now damping coefficient can be calculated with the following formula:

$$k_{dx} = 2d_x T_x k_{px} \tag{56}$$

It has the following value: $k_{dx} = 2 \cdot 0.707 \cdot 66.56 \cdot 6.366 \cdot 10^{-4}$ s · Nm/rad = 0.06 Nms/rd.

Finally, K_{px} and K_{dx} can be calculated. They are as follows: $K_{px} = \frac{k_{px}}{B_z k_{TRy}} = \frac{6.366 \cdot 10^{-4} Nm/rad}{2.86 \cdot 10^{-5} \cdot 1.25 T \cdot A \cdot m^2/V} = 17.8$ V/rad and $K_{dx} = \frac{k_{dx}}{B_z k_{TRy}} = \frac{0.06 Nms/rad}{2.86 \cdot 10^{-5} \cdot 1.25 T \cdot A \cdot m^2/V} = 1.678 \cdot 10^3 sV/rad.$

When T_x is determined, then the time constant for the differencing filter T_{fx} can be chosen from the condition that $T_{fx} << T_x$. In our example $T_x = 66.56$ s, let us take that $T_{fx} = 5$ s.

Simulation

Eqs. (51) and (52) were simulated using Simulink (see **Figure 29**).

Figure 29.
Satellite single-axis attitude control Simulink block scheme.

Blocks in the pink color present the satellite model, the dark green color is for control law blocks, the cyan blocks are registration oscilloscopes, and the display and the orange color are the disturbances. The red manual switch allows to implement the differentiating filter, transforming the scheme from the approximation (52) to the accurate presentation (51). Disturbing external torque M_d is constant; attitude sensor error is represented by the constant value ALP_0 and limited range white noise V that has spectral density $S_V = 2\sigma_V^2 T_v$ (σ_v is the standard deviation (SD), T_v is the correlation time). The results of the simulation (**Figure 29**) with and without the differentiating filter (with the assumption that $\dot{\alpha}_x \dot{\alpha}_x$ is directly measured without any errors) are presented below in **Figures 30–34** (left A, (52), without the filter; right B, (51), with the filter). The numerical data for the simulation are as follows:

$$J = 2.82 \text{ kgm}^2, T_x = \sqrt{\frac{J_x}{k_{px}}} = 66.56 \text{ s}, d_x = \frac{k_{dx}}{2T_x k_{px}} = 0.707,$$

$$k_{px} = 6.366 \cdot 10^{-4} \text{ Nm/rad}, k_{dx} = 0.06 \text{ Nm} \cdot \text{s/rad}, T_{fx} = 5 \text{ s},$$

$$M_d = 10^{-5} \text{Nm}, \Delta\alpha_{x0} = dltALP_0 = 0.1°, \Delta\alpha_{x0} = dltALP_0 = 0.1°$$

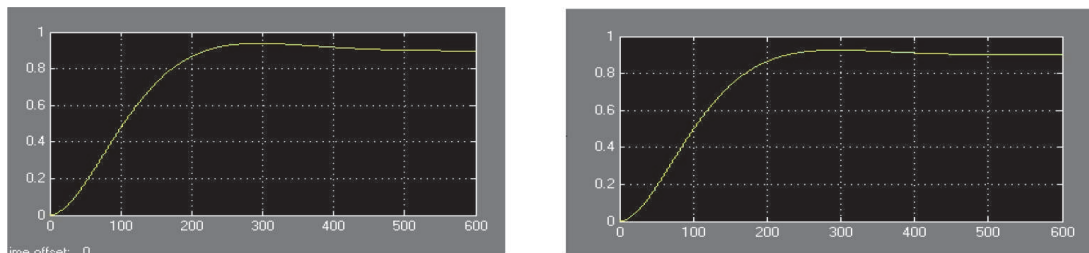Simulation of ACS (**Figure 29**) is presented in **Figures 30–34**. Units: vertical axis (deg), horizontal axis: (s).

(a)   (b)
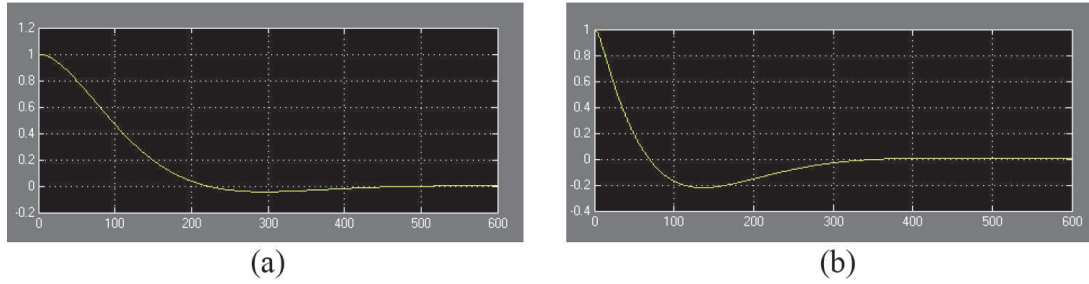
Figure 30.
Response to initial deviation angle $\alpha_{x0} = 1°$. (a) without dif. filter and (b) with dif. filter.
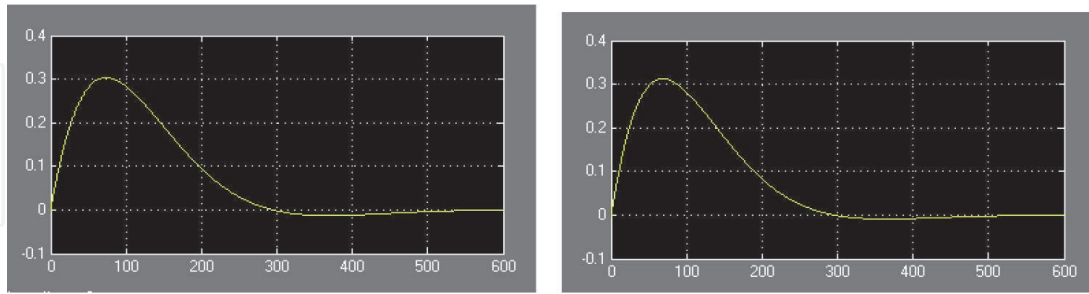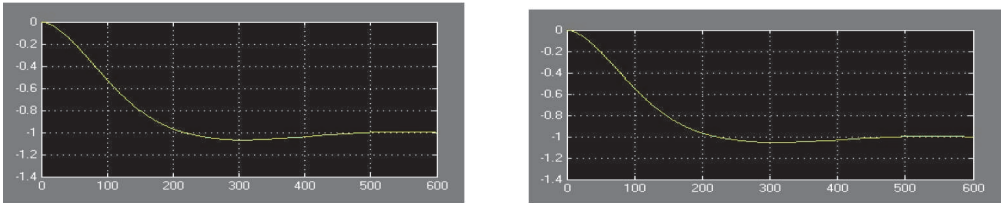

Figure 31.
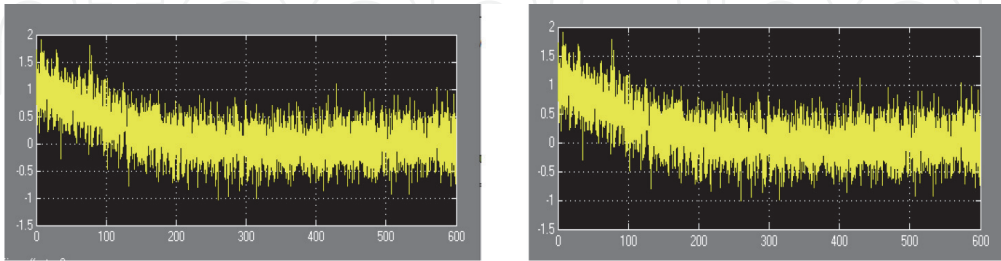*Response to initial angular velocity $\dot{\alpha}_{x0} = 0.01\text{deg/s}$.*

Figure 32.
Response to external disturbance torque $T_d = 10^{-5}\text{Nm}$. Static error $\alpha_x^* = 0.898°$.

Figure 33.
Response to attitude sensor bias $\Delta_{x0} = 1°$ plus white noise $\sigma_V = 0.1°$, $T_V = 1$ s. Satellite attitude stabilization errors, ALP.

Figure 34.
Satellite attitude measured errors ALPm.

Decay time: $\tau = 195s$, $\alpha_x(3\tau) = 5\%\alpha_{x0}$ (deg), (s) $\tau = 275s$.

As it can be seen, measured noise is filtered effectively in the control loop, and stabilization error is equal to the sensor bias with opposite sign.

In **Figure** 34, we can see that the measured (perceived) errors that TLM data provide to ground after the decay time do not present sensor bias and present only measured noise. It is because satellite stabilization error with opposite sign compensates the bias. In general, it can also be seen that the simulation of the approximate second-order model (52) is very close to the accurate model (51). Hence, at least for the analytical representation, (52) can be successfully used.

4. Conclusion

Part I of this chapter presents an overview of practical satellite control system, satellite guidance, navigation and control equipment. The work presented here is based on the author's point of view of integration of this GN&C equipment in the integrated AODCS system (satellite GN&C Spacetronics System). Main work principles, architecture, and components of the satellite control system were briefly highlighted.

The chapter can serve to a wide pool of space system specialists as an introduction to satellite control system development.

Acknowledgements

experience and background in Aerospace Technology were also accumulated from the former USSR (Moscow Aviation Institute, Moscow Aviapribor Corporation, Moscow Experimental Design Bureau Mars, Institute in Problems in Mechanic of RAN) and Israel (IAI, Lahav Division and Tashan Engineering Center), where he could observe and learn from diverse and wealthy engineering and scientific schools led by great scientists and designers such as Prof. BA. Riabov, Prof. V.P. Seleznev, V.A. Yakovlev, G. I. Chesnokov, V.V. Smirnov, Dr. A. Syrov, Acad. F. Chernousko, A. Sadot and Dr. I. Soroka.

This chapter was written as a solo author since his friend and regular coauthor Prof. George Vukovich from York University of Toronto passed away 2 years ago. For many years, Prof. Vukovich served as Director of his Department of Spacecraft Engineering in CSA. He will always keep good memories of Prof. Vukovich who helped and encouraged him continue his scientific and engineering work.

The author also acknowledges the copyrights of all publishers of the illustrations that were extracted from the open sources in the Internet.

Note

Dedicated to Prof. G. Vukovich.

Author details

Yuri V. Kim
David Florida Laboratory, Canadian Space Agency (CSA), St. Hubert, Ottawa, Canada

*Address all correspondence to: yurikim@hotmail.ca

IntechOpen

References

[1] Eickhoff J. On Board Computers, on Board Software and Satellite Operation. Berlin: Springer-Verlag; 2012

[2] Space Systems, Design, Qualification and Acceptance Tests of Small Spacecraft and Units. International Standard, ISO 19683; 2017

[3] Space Engineering, Satellite Attitude and Orbital Control System (AOCS) Requirements, ECSS-E-ST-60-30C; 2013

[4] Development of First Artificial Satellites (Rus.). Available from: https://www.kik-sssr.ru/Hist_1_PS-1_books.htm [Accessed: 15 January 2020]

[5] Available from: https://www.space.com 17563-sputnik. Sputnik: The Space Race's Opening Shot [Accessed: 17 January 2020]

[6] Chaturvedi A. Do You Know How Many Satellites Are Currently Orbiting Around the Earth? Available from: https://www.geospatialworld.net/blogs/do-you-know-how-many-satellites-earth/ [Accessed: 16 January 2020]

[7] About the David Florida Laboratory-Canada.ca, Available from: https://www.asc-csa.gc.ca/eng/laboratories-and-warehouse/david-florida/about.asp [Accessed: 17 January 2020]

[8] Delchamos T, Jonason G, Swift R. The Spacecraft Test and Evaluation Program, Telestar I, NASA SP-32. Washington, DC; 1963. p. 1007

[9] Sidi M. Spacecraft Dynamics and Control. A Practical Engineering Approach. Cambridge: Cambridge University Press; 1997

[10] Wertz JR, editor. Spacecraft Attitude Determination and Control. Dordrech: Kluwer Academic Publishers; 1978

[11] You Z. Space Microsystems and Micro/Nanosatellites, National Defence Industry Press. NY: Elsevier Inc; 2018

[12] Lee J, de Rouiter A, Ng A, Lambert C, Kim Y, Yoshihara K. Attitude Determination and Control Subsystem of JC2Sat-FF Mission. In: Proceedings of 12th International Aerospace Conference ISCOPS in Montreal, July 2010, AAS 10-427; 2010

[13] Bryson AE, Yu-Chi Ho J. Applied Optimal Control. Levittown, PA: Taylor & Francis; 1975. pp. 364-373, 369, 457

[14] Fourati H, Belkhiat D. Multisensor Attitude Estimation. Fundamental Concepts and Applications. NW: CRC Press, Taylor & Francis Group; 2017

[15] Kim YV. Kalman filter decomposition in the time domain using observability index, IFAC, Seoul, July 6–11, 2008. In: International Conference Proceedings. Vol. 2. NY: Curran Associates Inc.; 2009. pp. 625-630

[16] Seleznev VP. Navigation Devises, Rus. Moscow: Mashinistroenye; 1974

[17] Chatfield A. Fundamentals of High Accuracy Inertial Navigation. Reston, VA: AIAA; 1974

[18] Titterton D, Weston J. Strapdown Inertial Navigation Technology. Reston, VA: The Institute of Engineering and Technology; 1996

[19] Hofmann-Welenghof B, Lichtenegger H, Collins J. GPS Theory and Practice. New York: Springer-Verlag Wien; 2001

[20] Shuster M, Oh S. Three-axis attitude determination from vector observations. Journal of Guidance & Control. 1981;**4**(1):70-77

[21] Armenise M, Ciminelli C, Dell'Olio F, Passaro V. Advances in Gyroscope Technologies. Berlin: Springer-Verlag; 2010

[22] Arnold R, Maunder L. Gyrodynamics and its Engineering Applications. London: Academic Press; 1961

[23] Meshchersky IV. Dynamics of a point of variable mass. In: Work on the Mechanics of Bodies of Variable Mass. 2nd ed. GITTL, Moscow; 1952. pp. 37-188, 280

[24] A Man- and an Equation, ESA. Available from: http://blogs.esa.int/ rocketscience/2012/10/14/a-man-and-an-equation/ [Accessed: 19 January 2020]

[25] How to Slow Down Satellite Rotation? D-dot Algorithm, ESE 3 Sat Project. Available from: http://www. ece3sat.com/blog/2018-01-25-how-to-slow-down-rotation-the-bdot-algorithm/

[26] Space Engineering-Software, ECSS-E-ST-40C, Noordwijk; 2019

[27] Vukovich G, Kim Y. Satellite orbit deacay due to atmospheric drag. International Journal of Space Science and Engineering. Inderscience Publishers; 2019;**5**(2). Availabe from: www.inderscience.com/jhome.php?/jcode=ijspacese. [Acessed: 4 June 2020]